ARTHRITIS & RHEUMATISM
Vol. 65, No. 11, November 2013, pp 2857–2865
DOI 10.1002/art.38114

Periarticular Bone Loss in Antigen-Induced Arthritis

Cecilia Engdahl, Catharina Lindholm, Alexandra Stubelius, Claes Ohlsson, Hans Carlsten, and Marie K. Lagerquist

Objective. **Bone loss in arthritis is a complex process characterized by bone erosions and periarticular and generalized bone loss. The antigen-induced arthritis (AIA) model is mainly used to study synovitis and joint destruction, including bone erosions; however, periarticular bone loss has been less extensively investigated. The objectives of this study were to characterize and establish AIA as a model for periarticular bone loss, and to determine the importance of NADPH oxidase 2 (NOX-2)–derived reactive oxygen species (ROS) in periarticular bone loss.**

Methods. **Arthritis was induced in mice by local injection of antigen in one knee; the other knee was used as a nonarthritis control. At study termination, the knees were collected for histologic assessment. Periarticular bone mineral density (BMD) was investigated by peripheral quantitative computed tomography. Flow cytometric analyses were performed using synovial and bone marrow cells.**

Results. **AIA resulted in decreased periarticular trabecular BMD and increased frequencies of preosteoclasts, neutrophils, and monocytes in the arthritic synovial tissue. Arthritis induction resulted in an increased capability to produce ROS. However, induction of arthritis in Ncf1*/* mice, which lack NOX-2–derived ROS, and control mice resulted in similar reductions in periarticular trabecular BMD.**

Conclusion. **The initiation of AIA resulted in periarticular bone loss associated with local effects on inflammatory cells and osteoclasts. Furthermore, based on our observations using this model, we conclude that NOX-2–derived ROS production is not essential for inflammation-mediated periarticular bone loss. Thus, AIA can be used as a model to investigate the pathogenesis of local inflammation–mediated bone loss.**

Inflammatory arthritis is characterized by massive infiltration of mononuclear and polymorphonuclear cells into the joints, resulting in synovitis, destruction of articular cartilage, and bone loss (1). Such bone loss includes 1) bone erosions affecting the subchondral bone and bone at the joint margins, 2) periarticular bone loss adjacent to the inflamed joints, and 3) generalized osteoporosis (2,3). Periarticular bone loss is a characteristic feature of early arthritis but has not been studied as extensively as bone erosions and generalized osteoporosis.

The mechanisms involved in inflammation-mediated bone loss in arthritis are only partly understood, and several different cell types are implicated. Osteoclasts, derived from hematopoietic stem cells, are responsible for bone resorption. The presence of macrophage colony-stimulating factor (M-CSF) leads to increased proliferation and survival of osteoclast precursor cells, as well as up-regulated expression of RANK in these cells (4). RANKL, which is expressed by synovial fibroblasts (5), osteoblasts (6), osteocytes (7), and activated Th cells (8), stimulates RANK, which leads to osteoclast formation (9). The interaction between RANK and RANKL is inhibited by the decoy receptor osteoprotegerin (OPG), which is ubiquitously expressed.

Supported by the Ragnar Söderberg Foundation, the Medical Faculty of the University of Gothenburg, the Gothenburg Medical Society, the Rheuma Research Fund Margareta, COMBINE, the Swedish Research Council, King Gustav V's 80-Year Foundation, the Association Against Rheumatism, the Swedish Association for Medical Research, LUA/ALF, and the Åke Wiberg Foundation.

Cecilia Engdahl, PhD, Catharina Lindholm, MD, PhD, Alexandra Stubelius, MSc, Claes Ohlsson, MD, PhD, Hans Carlsten, MD, PhD, Marie K. Lagerquist, PhD: University of Gothenburg, Gothenburg, Sweden.

Address correspondence to Cecilia Engdahl, PhD, Centre for Bone and Arthritis Research, Department of Rheumatology and Inflammation Research, Institute of Medicine, University of Gothenburg, Box 480, 405 30 Gothenburg, Sweden. E-mail: cecilia.engdahl@gu.se.

Submitted for publication March 15, 2013; accepted in revised form July 25, 2013.

The presence of M-CSF and RANKL is essential for osteoclastogenesis to occur; however, osteoclastic bone resorption is enhanced by inflammatory cytokines such as tumor necrosis factor α (TNFα), interleukin-6 (IL-6), IL-1, and IL-17 (10–13). Synovial macrophages are also important in inflammation-mediated bone loss due to their prominent number in inflamed synovial tissue and are, together with neutrophils, key cells producing inflammatory cytokines and chemokines that attract and activate T cells (14,15). Activated Th cells comprise a large proportion of the invading cells in inflamed synovial tissue and may therefore be of importance in pathogenesis (16,17). Th17 cells, a subgroup of the Th cells implicated in the pathogenesis of arthritis (18), produce the inflammatory cytokines IL-17 and RANKL, both of which are important in osteoclastogenesis.

The roles of NADPH oxidase (NOX) and reactive oxygen species (ROS) in autoimmune diseases such as rheumatoid arthritis (RA) have been intensively studied (19). Neutrophils and macrophages phagocytize antigens and, as a direct response, produce ROS, which are essential for the activation of proteolytic enzymes and the prevention of antigen diffusion (20). ROS are well-known immune promoters (21), and it has been shown, experimentally, that excessive production of ROS may lead to accelerated joint destruction and osteoclast activation (22–24). However, it has also been shown that limited ROS production in *Ncf1*-mutated mice, caused by impaired NOX-2 function, results in enhanced disease severity in several different animal models of arthritis (25,26). Thus, the exact role of ROS in arthritis is not completely understood.

In the present study, we used the antigen-induced arthritis (AIA) model to examine the influence of inflammatory arthritis on periarticular bone loss. This model is characterized by leukocyte infiltration and synovitis, together with bone and cartilage destruction, and shows several clinical and histopathologic features similar to those in human RA (27). The aim of this study was to investigate periarticular bone loss in AIA and to study the associated effects on local cellular distribution in bone marrow and synovial tissue. Finally, we used the AIA model to determine the importance of NOX-2–derived ROS in periarticular bone loss.

MATERIALS AND METHODS

Animals. The ethics committee for animal experiments at the University of Gothenburg approved this study. Female B.10QNcf1$^{*/*}$ mice with a point mutation in the Ncf1 gene (26), corresponding control B.10Q mice, and C57/BL6 mice (Scanbur) were maintained (5–10 mice per cage) under standard environmental conditions and fed standard laboratory chow and tap water ad libitum.

Induction of arthritis. C57/BL6, B.10QNcf1$^{*/*}$, and B.10Q mice were immunized with 0.2 mg of murine bovine serum albumin (mBSA; Sigma-Aldrich) dissolved in phosphate buffered saline (PBS) and emulsified with an equal volume of Freund's complete adjuvant (Sigma-Aldrich). A total volume of 100 μl was injected intradermally at the base of the tail (50 μl on each side). After 7 days, the mice received a second injection of 0.3 mg of mBSA dissolved in 30 μl of vehicle (20% distilled H_2O, 80% saline) into the knee joint (arthritic side). The other knee was injected with vehicle and used as an internal control (nonarthritic side). A comparison of C57/BL6 mice with AIA and C57/BL6 mice without AIA (naive mice) was performed to control for systemic effects of the mBSA injection. In the naive mice, saline was used for both the intradermal and the local knee injections.

Histologic examination. Fourteen days after the primary immunization, the mice were anesthetized with ketamine/medetomidine (Pfizer), bled, and killed by cervical dislocation. Knees from the C57/BL6, B.10QNcf1$^{*/*}$, and B.10Q mice were separately placed in 4% formaldehyde, decalcified, and embedded in paraffin. Sections were stained with hematoxylin and eosin, and an examiner (CE) graded synovitis and joint destruction in a blinded manner. Synovial hypertrophy was defined as a membrane thickness of >2 cell layers (28). A histologic scoring system was used, where 1 = mild, 2 = moderate, and 3 = severe.

Determination of periarticular bone mineral density (BMD). To determine periarticular bone loss, the skin was removed from both legs (arthritic and nonarthritic), and both the femur and tibia were analyzed using Stratec pQCT XCT Research M software version 5.4B (Norland) at a resolution of 70 μm, as described previously (29). Total, trabecular, and subcortical BMD were determined with metaphyseal scanning performed 0.4 mm from the growth plate, in the proximal direction in the femur and in the distal direction in the tibia. The inner 45% of the bone area was defined as the trabecular bone compartment, and the subcortical–cortical bone compartment was defined as bone with a density of >400 mg/cm^3. Cortical BMD was determined with mid-diaphyseal scanning.

Osteoclast staining. Osteoclast numbers in the femur and tibia epiphyses were determined using cathepsin K antibodies (30). Knee joints were placed in formaldehyde, decalcified, and embedded in paraffin. Sections were cut and treated with H_2O_2, protein block (Dako), and an Avidin/Biotin Blocking Kit (Vector). Sections were stained with polyclonal rabbit anti–cathepsin K primary antibodies (1:200 dilution; Abcam), and normal rabbit serum (Dako) was used as a negative control. A secondary horse anti-rabbit antibody was used, followed by incubation with peroxidase substrate (ImmPRESS Reagent Kit and ImmPACT AEC kit; Vector). All sections were counterstained with Mayer's hematoxylin (Histolab). The slides were coded, and the number of osteoclasts (multinucleated cathepsin K–positive cells) per 0.1 mm^2 in the epiphysis was counted.

Tissue collection and flow cytometry. Synovial tissue from 2 arthritic or 2 nonarthritic knees was pooled and placed in RPMI medium (Fisher Scientific). The tissue was resuspended in medium with DNase I (Sigma-Aldrich) and type IV collagenase (Roche) and incubated for 1 hour at 37°C. A

single-cell suspension was obtained after the tissue was mashed and passed through a 40-μm cell strainer (Becton Dickinson) in 4 ml PBS. Three draining lymph nodes from the arthritic and nonarthritic legs were examined and placed in cold PBS. A single-cell suspension was obtained after the tissue specimens were mashed and passed through a 30-μm cell strainer (Becton Dickinson) in 1 ml PBS. Bone marrow cells were harvested from 4 bone compartments per mouse (the distal and proximal parts of the femur from both the arthritic and nonarthritic sides), using a syringe with 5 ml of PBS. The spleens were examined, and single-cell suspensions were obtained after the tissue was mashed and passed through a 70-μm cell strainer (Becton Dickinson) in 15 ml PBS. Pelleted cells from bone marrow and spleen were resuspended in Tris-buffered 0.83% NH_4Cl solution, to lyse erythrocytes, and washed in PBS. The total number of leukocytes was analyzed using an automated cell counter (Sysmex).

Cells from spleen, synovial tissue, lymph nodes, and bone marrow were analyzed using the following antibodies: allophycocyanin (APC)– or APC–Cy7–conjugated anti-F4/80 (BioLegend), BD Horizon V450–conjugated anti-CD11b (Becton Dickinson), fluorescein isothiocyanate (FITC)–conjugated anti-CD3 (Becton Dickinson), BD Horizon V450–conjugated anti-CD4 (Becton Dickinson), FITC-conjugated anti-CD8 (Becton Dickinson), PerCP-conjugated anti-CD19 (BioLegend), phycoerythrin-conjugated anti–Gr-1 (Becton Dickinson), and APC-conjugated anti–colony-stimulating factor receptor (BioLegend).

Intracellular ROS production was determined using dihydrorhodamine 123 dye (Invitrogen), which, after oxidization by ROS, forms the highly fluorescent product rhodamine 123. Formation of rhodamine 123 is monitored by fluorescence excitation and emission wavelengths of 500–536 nm. To quantify the respiratory burst activity, the cells were incubated at 37°C for 15 minutes, in the presence or absence of phorbol myristate acetate (PMA; Sigma-Aldrich). The increase in intracellular respiratory burst activity was determined as the measurement of rhodamine 123 in PMA-stimulated neutrophil and monocyte/macrophage populations minus unstimulated cells (in the same population).

Cells were analyzed using a FACSCanto II system (Becton Dickinson). FlowJo version 8.5.2 software (Tree Star) was used to analyze the data.

Real-time polymerase chain reaction (PCR). RNA was isolated from the homogenate of 2 pooled synovial tissue specimens (from 2 individual mice), draining lymph nodes, bone marrow cells, trabecular bone (the femur epiphysis, containing a minor proportion of articular cartilage and cortical bone), and cortical bone (the femur diaphysis) from both the arthritic and the nonarthritic sides, using an RNeasy kit (Qiagen). The amplifications were performed using a StepOnePlus Real-Time PCR System (PE Applied Biosystems), with Assay-on-Demand primer and probe sets (PE Applied Biosystems) labeled with the reporter fluorescent dye FAM. Predesigned primers and a probe labeled with the reporter fluorescent dye VIC, specific for 18S ribosomal RNA (rRNA), was included as an internal standard. The assay identification numbers were as follows: for RANK, Mm00437135_m1; for RANKL, Mm00441908_m1; for OPG, Mm00435452_m1; for M-CSF, Mm00432686_m1; for IL-17A, Mm00439618_m1; for IL-1β, Mm00434228_m1; for IL-6, Mm0046190_m1; and for TNFα, Mm00443258_m1. The amount of messenger RNA for each gene was calculated using a standard curve method according to the manufacturer's instructions (PE Applied Biosystem) and adjusted for 18S rRNA.

Statistical analysis. Student's paired *t*-test was used for comparisons within mice (arthritic side versus nonarthritic side), and Student's unpaired *t*-test was used for comparisons between mice. Histologic scoring was performed using an ordinal scale system requiring nonparametric statistical evaluation; therefore, a Mann-Whitney test was used. Statistical calculations were performed using GraphPad Prism Mac 6.0d. *P* values less than 0.05 were considered significant.

RESULTS

Synovitis and joint destruction in the arthritic joints of mice. Severe arthritis developed in the antigen-injected knee joints, as revealed by massive cellular infiltration into the joint space, synovial inflammation, and joint destruction (Figures 1A and B). In contrast, histologic examination of the nonarthritic joints showed no synovial inflammation or joint destruction. The joints from naive nonarthritic mice (in which saline was injected both intradermally and into both knees) showed no signs of either synovial inflammation or joint destruction (data not shown).

Periarticular bone loss and increased osteoclast numbers after AIA induction. BMD in the femur and tibia, on both the arthritic and nonarthritic sides, was assessed using peripheral quantitative computed tomography (QCT). The induction of arthritis was associated with a decrease in total BMD in the metaphyseal region of both the distal femur (-13%; $P < 0.001$) and the proximal tibia (-7%; $P < 0.001$). This decrease was associated with a decrease in trabecular BMD in both the distal femur and proximal tibia (-30% [$P < 0.001$] and -33% [$P < 0.001$], respectively) (Figures 1C and D), while no change in subcortical–cortical BMD was detected (data not shown). Mid-diaphyseal scanning showed no effect of arthritis induction on cortical BMD, in either the tibia or the femur (Figure 1E). Trabecular and cortical BMD in the femur and tibia on the nonarthritic side of mBSA-injected mice were similar to the BMD in the femur and tibia of naive mice that were injected with saline (data not shown). Immunohistochemistry was used to determine the number of osteoclasts in the epiphyseal parts of the femur and tibia on the arthritic side compared with the nonarthritic side. Cathepsin K staining of the joint showed a significant increase in the number of osteoclasts in the epiphyseal region of both the tibia ($+71\%$; $P < 0.001$) and the femur ($+90\%$; $P < 0.05$) on the arthritic side compared with the nonarthritic side (Figure 1F).

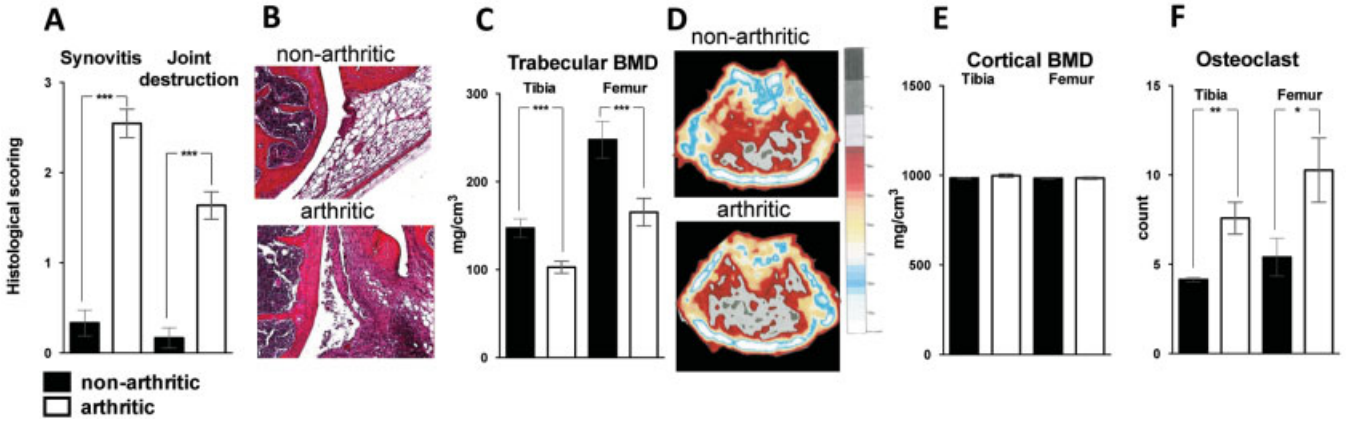

Figure 1. Synovitis, joint destruction, and periarticular bone loss in mice with antigen-induced arthritis. **A,** Histologic scores for synovitis and joint destruction in arthritic and nonarthritic knees. Values are the mean ± SEM (n = 13 mice per group). *** = $P < 0.001$ by Mann-Whitney U test. **B,** Representative images of histologic sections from arthritic and nonarthritic knee joints. **C,** Trabecular bone mineral density (BMD) in the metaphyseal region, as determined by peripheral quantitative computed tomography (QCT). Values are the mean ± SEM (n = 13 mice per group). *** = $P < 0.001$ by Student's paired *t*-test. **D,** Representative peripheral QCT images showing cross-sections of the metaphyseal region of the femur. The grayscale represents bone density, from 0 (black) to 750 mg/cm^3 (white). **E,** Cortical BMD in the diaphyseal region. Values are the mean ± SEM (n = 13 mice per group). **F,** Osteoclast count in the tibia and femur (per 0.1 mm^2), on the arthritic side and the nonarthritic side. Values are the mean ± SEM (n = 8 mice per group). * = $P < 0.05$; ** = $P < 0.001$ by Student's paired *t*-test.

Increased frequency of inflammatory cells in synovial tissue from arthritic knees. The synovial cell populations in arthritic and nonarthritic knees were investigated using flow cytometry. Arthritic synovial tissue showed an increased frequency of neutrophils, monocyte/macrophages, and T cells (+201%, +121%, and +75%, respectively; $P < 0.05$) compared with nonarthritic synovial tissue (Figures 2A–C). No difference in B cell frequencies was observed (Figure 2D). These findings suggested that neutrophils, monocyte/macrophages, and T cells are recruited to arthritic synovial tissue.

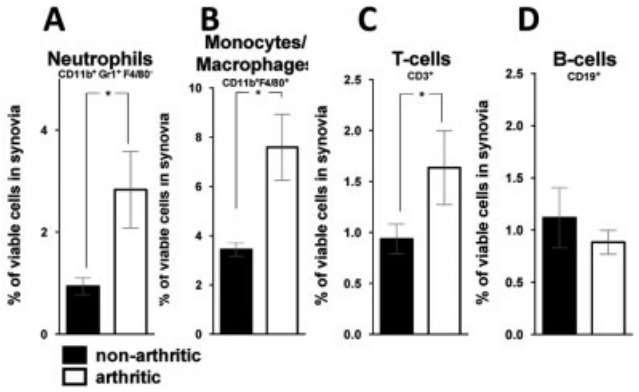

Figure 2. Frequencies of neutrophils (**A**), monocyte/macrophages (**B**), T cells (**C**), and B cells (**D**) in arthritic and nonarthritic mouse knees. Values are the mean ± SEM (n = 8 mice per group). * = $P < 0.05$ by Student's paired *t*-test.

Increased frequencies of preosteoclasts, neutrophils, and monocyte/macrophages in bone marrow from the distal, but not the proximal, part of the femur on the arthritic side. Bone marrow cell populations in the distal and proximal parts of the femur were investigated using a cell counter and flow cytometry. In the distal part of the femur, the bone marrow cell number was increased on the arthritic versus the nonarthritic side (+12%; $P < 0.01$) closest to the inflammation, while no difference in the bone marrow cell number was detected when comparing the proximal parts. Bone marrow from the distal part of the femur on the arthritic side displayed increased frequencies of preosteoclasts (+33%; $P < 0.01$) (Figure 3A), neutrophils (+7%; $P < 0.05$) (Figure 3B), and monocyte/macrophages (+6%; $P < 0.01$) (Figure 3C) compared with the nonarthritic side. No differences in the numbers of T cells or B cells were detected (Figures 3D and E). Interestingly, there were no differences in any cell population between the nonarthritic and arthritic sides in the proximal part (Figure 3), suggesting a very local effect on bone marrow cellularity and cell distribution.

Effect of AIA on the gene expression pattern in the vicinity of the arthritic joint. The expression of bone-associated genes in synovial tissue, bone marrow, trabecular bone, and cortical bone from the arthritic side

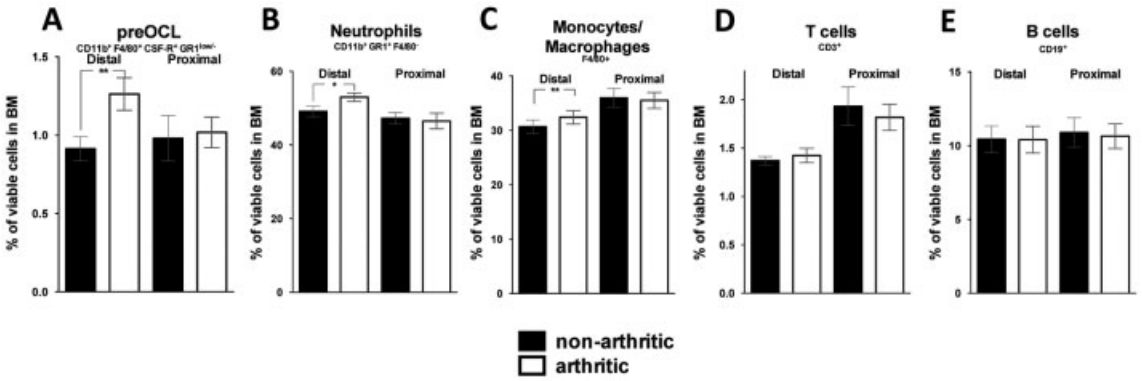

Figure 3. Frequencies of preosteoclasts (preOCL) (**A**), neutrophils (**B**), monocyte/macrophages (**C**), T cells (**D**), and B cells (**E**) in bone marrow (BM) from the distal and proximal parts of the femur on the arthritic side compared with the nonarthritic side. Values are the mean ± SEM (n = 8 mice per group). CSF-R = colony-stimulating factor receptor. ∗ = $P < 0.05$; ∗∗ = $P < 0.01$ by Student's paired *t*-test.

was compared with that in the nonarthritic side. RANK, RANKL, and M-CSF expression was induced in arthritic synovial tissue, bone marrow, and trabecular bone (Table 1). OPG expression was significantly reduced in arthritic synovia but was not significantly altered in bone marrow or the bone compartments (Table 1). No alterations in the expression of these bone-associated genes (RANK, RANKL, and M-CSF) were detected in cortical bone (Table 1).

The expression of inflammation-associated genes in synovial tissue, bone marrow, trabecular bone, cortical bone, and draining lymph nodes from the arthritic side was compared with that in the nonarthritic side. Expression of IL-17A, TNFα, IL-6, and IL-1β in synovial tissue and bone marrow was increased in the arthritic side compared with the nonarthritic side (Table 1). TNFα was also increased in trabecular bone (Table 1). No differences in the expression of inflammation-associated genes were seen in either draining lymph nodes or cortical bone from the arthritic side versus the nonarthritic side (Table 1).

Systemic immune responses in mice with AIA and naive mice. Splenocytes from mBSA-injected mice showed no alteration in the cellularity or frequency of immune cells, including monocyte/macrophages, neutrophils, and lymphocytes, compared with splenocytes from naive mice injected with saline (data not shown). The counts and frequencies of the inflammatory cells investigated were similar in draining lymph nodes from the arthritic side and those from the nonarthritic side (data not shown).

Induction of intracellular ROS production in myeloid bone marrow cells from the distal, but not the proximal, part of the femur on the arthritic side. Respiratory burst activity was investigated in bone marrow from the proximal and distal parts of the femur, on

Table 1. Gene expression in synovial tissue, bone marrow, and trabecular bone after induction of arthritis*

	Synovial tissue	Bone marrow	Draining lymph node	Trabecular bone	Cortical bone
Bone-associated genes					
RANK	148 ± 40†	34 ± 15‡	–	82 ± 39†	−16 ± 15
RANKL	442 ± 188†	118 ± 47‡	–	73 ± 43†	−20 ± 10
Osteoprotegerin	−68 ± 4†	125 ± 87	–	70 ± 28	−5 ± 22
M-CSF	48 ± 30†	41 ± 12†	–	140 ± 70†	−18 ± 9
Inflammation-associated genes					
Interleukin-17A	40 ± 13†	60 ± 24†	−4 ± 11	ND	ND
Tumor necrosis α	176 ± 39‡	43 ± 19†	6 ± 23	79 ± 41†	3 ± 20
Interleukin-6	41 ± 14‡	338 ± 108†	1,547 ± 1,394	19 ± 13	−13 ± 23
Interleukin-1β	302 ± 171†	72 ± 42†	49 ± 40	186 ± 176	−16 ± 17

* Values are the mean ± SEM percent change in gene expression on the arthritic side compared with the nonarthritic side (n = 8–12 mice per group). M-CSF = macrophage colony-stimulating factor.
† $P < 0.05$ by Student's paired *t*-test.
‡ $P < 0.01$ by Student's paired *t*-test.

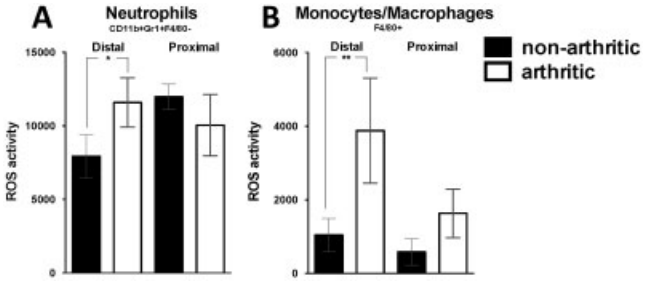

Figure 4. Respiratory burst activity in bone marrow cells from the arthritic and nonarthritic sides of the femur. The increase in respiratory burst activity in the distal and proximal regions of the femur was determined as the measurement of rhodamine 123 in phorbol myristate–stimulated cells in neutrophil (**A**) and monocyte/macrophage (**B**) populations minus the measurement in unstimulated cells (in the same population). Values are the mean ± SEM (n = 8 mice per group). $* = P < 0.05$; $** = P < 0.01$ by Student's paired *t*-test.

both the arthritic side and the nonarthritic side. Bone marrow from the distal part of the femur on the arthritic side showed increased respiratory burst activity in both neutrophils (+46%; $P < 0.05$) (Figure 4A) and monocyte/macrophages (+272%; $P < 0.01$) (Figure 4B) compared with the nonarthritic side. There was no change in respiratory burst activity in the proximal part of the femur in the arthritic side compared with the nonarthritic side (Figure 4). Thus, we concluded that the increase in respiratory burst activity caused by the induction of arthritis is a local event.

Role of NOX-2–derived ROS in periarticular bone loss in mice with AIA. To determine the importance of NOX-2–dependent ROS production in periarticular bone loss, arthritis was induced in B.10QNcf1$^{*/*}$ mice and control B.10Q mice. In both B.10QNcf1$^{*/*}$ mice and control B.10Q mice, severe synovitis and joint destruction developed in the arthritic knee joints, while the nonarthritic joints showed limited synovial inflammation and no joint destruction (Figures 5A and B). Periarticular trabecular BMD was decreased in the metaphyseal region of both the tibia and femur on the arthritic side (−22% and −37%, respectively; $P < 0.01$) compared with the nonarthritic side in control B.10Q mice. A similar decrease was observed in the femur and tibia on the arthritic side (−27% and −19%, respectively; $P < 0.001$) compared with the nonarthritic side in B.10QNcf1$^{*/*}$ mice (Figures 5C and D).

DISCUSSION

Bone loss in arthritis is a complex physiologic process and is dependent on several different cell types and cytokines. The inflammation in arthritic diseases may result in different types of bone loss and can cause both generalized bone loss, i.e., osteoporosis, as well as local bone loss, including bone erosions and periarticular osteopenia (2). The exact mechanism behind inflammation-mediated bone loss is not clearly understood and needs to be further studied in order to

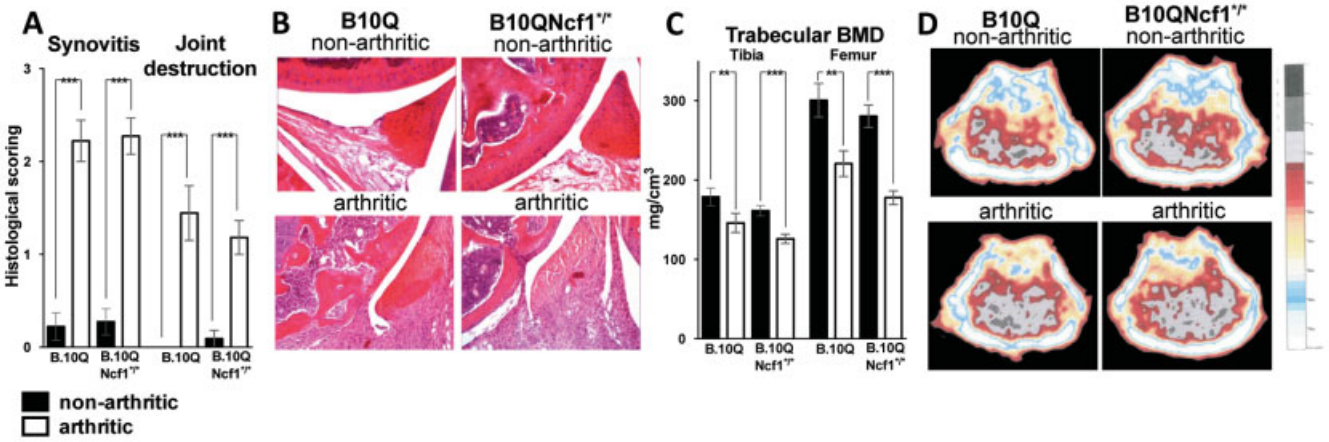

Figure 5. Effect of NADPH oxidase 2–derived reactive oxygen species on periarticular bone loss in *Ncf1*-mutated (B.10QNcf1$^{*/*}$) mice and control (B.10Q) mice with antigen-induced arthritis. **A,** Histologic scores for synovitis and joint destruction in arthritic and nonarthritic knees. Values are the mean ± SEM (n = 9–11 mice per group). $*** = P < 0.001$ by Mann-Whitney U test. **B,** Representative images of histologic sections from the metaphyseal region of the femur. **C,** Trabecular bone mineral density (BMD) in the tibia and femur. Values are the mean ± SEM (n = 9–11 mice per group). $** = P < 0.01$; $*** = P < 0.001$ by Student's paired *t*-test. **D,** Representative peripheral quantitative computed tomography images showing cross-sections of the metaphyseal region of the femur. The grayscale represents bone density, from 0 (black) to 750 mg/cm^3 (white).

facilitate the development of new arthritis-preventing drugs. Several different experimental models are available to study the pathogenesis of arthritis. The murine model of AIA results in local monarthritis, with no generalized bone loss, and has mainly been used to study the pathophysiology underlying synovitis and joint destruction, including bone erosions. In contrast, periarticular bone loss in AIA has been less extensively investigated.

In the current study, we used computed tomography to investigate the effect of AIA on periarticular bone loss. We also evaluated the impact of inflammation on 1) various cell types in synovial tissue, 2) local effects on inflammatory cells in bone marrow, 3) local effects on ROS production in bone marrow, and 4) gene expression in different joint-associated compartments. Furthermore, we used the AIA model to determine the importance of NOX-2–derived ROS for periarticular bone loss.

AIA has many histologic features of RA, including infiltration of inflammatory cells into the joint, synovitis, and joint destruction (27), and has been shown to be dependent on Th cells as well as synovial macrophages and neutrophils but independent of cytotoxic T cells and B cells (31–33). In accordance with this, we observed clear synovitis and joint destruction after the initiation of AIA and increased frequencies of monocyte/macrophages, neutrophils, and T cells in synovial tissue from arthritic knees compared with nonarthritic knees. Furthermore, expression of the cytokines IL-17A, TNFα, IL-6, and IL-1β was induced in arthritic synovial tissue but not nonarthritic synovial tissue. Induction of these cytokines in synovial fluid from patients with RA has been associated with disease activity (34–36). We also observed a significant decrease in periarticular trabecular BMD in both the distal femur and proximal tibia on the arthritic side versus the nonarthritic side, using peripheral QCT.

Periarticular bone loss in the rat model of AIA has been observed using histomorphometry (37). Similar to the findings of that study, we detected changes only in the trabecular and not in the cortical bone compartment in the metaphyseal regions of the distal femur and proximal tibia; no effects were seen in cortical BMD in the diaphyseal part of the femur or tibia. Trabecular bone has a more porous structure and remodels more actively than cortical bone and therefore is more susceptible to changes such as physiologic status, diet, or drug treatment. It has also been shown that biologic differences between trabecular and cortical bone can be characterized using quantitative PCR (38–40). In the current study, we observed significant up-regulation of the osteoclastogenesis-related genes RANKL, RANK, and M-CSF in trabecular but not cortical bone in the arthritic side compared with the nonarthritic side.

The inflammation-mediated bone loss was associated with an increased frequency of osteoclast precursors in bone marrow and an increased number of osteoclasts in the epiphyseal regions of the distal femur and proximal tibia. It has been suggested that mediators originating from inflammatory tissue affect osteoclasts by paracrine mechanisms, because the number of osteoclasts dramatically decreases with growing distance from the affected joint (41). In accordance with this, we detected effects on the frequency of preosteoclasts only in bone marrow from the distal part of the femur (closest to the inflamed joint) and not in bone marrow from the proximal part of the femur.

We next studied effects of arthritis on inflammatory cells in the bone marrow and observed that these cells were affected by inflammation in a local manner. The frequency of inflammatory cells in bone marrow from the distal but not the proximal part of the femur was increased in the arthritic side compared with the nonarthritic side, with increased frequencies of macrophages, neutrophils, and preosteoclasts in the area closest to the inflamed joint. Thus, inflammation has very local effects on bone marrow cells, suggesting that the factors mediating the effects signal in a paracrine manner. It is well known that there are variations in the transverse direction of bone marrow cell populations within a femur (42), but such differences in the longitudinal direction have not been previously recognized.

ROS are widely considered to be involved in several destructive conditions; however, ROS may have a dual role. High ROS production in pathologic conditions such as RA increases osteoclast activity, but ROS can also provide hyperoxidative stress and thereby induce apoptosis of osteoclasts (43). ROS have a primarily proinflammatory role in RA and mediate tissue damage, but low levels of ROS have been shown to have a regulatory function in arthritis (21,25). Circulating neutrophils and neutrophils in synovial fluid from patients with RA have increased ROS production due to higher NOX-2 activity (44,45). In accordance with this, we observed an increased capability of neutrophils and monocytes to produce intracellular ROS in bone marrow from the distal part of the femur, closest to the inflammation, but not from the proximal part. These data indicate that this effect of arthritis induction on ROS production is strictly local.

To determine the importance of ROS production

in periarticular bone loss, we used *Ncf1*-mutated mice, which are incapable of producing NOX-2–derived ROS. The Ncf1$^{*/*}$ mice displayed no difference compared with their controls regarding arthritis development, including synovitis and joint destruction or periarticular bone loss. Thus, we conclude that ROS production via NOX-2 is not mandatory for the development of arthritis or inflammation-mediated periarticular bone loss in AIA. Mutated *Ncf1* has previously been shown to both enhance (26) and reduce (46) arthritis severity in different murine models of arthritis compared with wild-type mice. Hence, ROS production can have different roles depending on the model used. NOX-2 is responsible for the majority of the ROS production, and the *Ncf1* mutation results in loss of detectable respiratory burst activity (21,26,47–49). However, we cannot exclude the possibility that minor ROS production by other oxidases may be involved in the inflammation-mediated bone loss observed in this model.

RA is a complex disease with high heterogeneity among patients (50), and currently there is no animal model of arthritis that totally reflects the pathogenesis. It is therefore important to choose the appropriate animal model in order to address the question being posed. We show that use of the AIA model is suitable to investigate local inflammation–mediated periarticular bone loss and propose that this model may be useful to increase knowledge regarding local bone loss, not only in RA, but also in other monarthritic diseases, including reactive arthritis and gout. This animal model makes it possible to compare the arthritic and nonarthritic joints in the same animal and is therefore ideal for investigating different antiarthritis therapies and their abilities to protect against local bone loss. Furthermore, the AIA model has no strain restrictions (50), and by using different genetically modified animals, which may be on different genetic backgrounds, the mechanisms behind local bone loss could be further elucidated.

In conclusion, AIA results in periarticular bone loss associated with local effects on inflammatory cells and osteoclasts. Furthermore, using this AIA model, we determined that NOX-2–derived ROS production is not essential for inflammation-mediated periarticular bone loss. Thus, AIA can be used as a model to investigate the pathogenesis of local inflammation–mediated bone loss, and increased knowledge of the pathophysiology behind such bone loss in arthritis may help in identifying beneficial therapeutic strategies to protect bone in inflammatory diseases.

ACKNOWLEDGMENTS

We thank Malin Erlandsson, Lotta Uggla, and Anette Hansevi for excellent technical assistance.

AUTHOR CONTRIBUTIONS

All authors were involved in drafting the article or revising it critically for important intellectual content, and all authors approved the final version to be published. Dr. Engdahl had full access to all of the data in the study and takes responsibility for the integrity of the data and the accuracy of the data analysis.

Study conception and design. Engdahl, Lindholm, Stubelius, Ohlsson, Carlsten, Lagerquist.

Acquisition of data. Engdahl, Stubelius, Lagerquist.

Analysis and interpretation of data. Engdahl, Lindholm, Stubelius, Carlsten, Lagerquist.

REFERENCES

1. Feldmann M, Brennan FM, Maini RN. Rheumatoid arthritis. Cell 1996;85:307–10.
2. Goldring SR, Gravallese EM. Mechanisms of bone loss in inflammatory arthritis: diagnosis and therapeutic implications. Arthritis Res 2000;2:33–7.
3. Deodhar AA, Woolf AD. Bone mass measurement and bone metabolism in rheumatoid arthritis: a review. Br J Rheumatol 1996;35:309–22.
4. Hayase Y, Muguruma Y, Lee MY. Osteoclast development from hematopoietic stem cells: apparent divergence of the osteoclast lineage prior to macrophage commitment. Exp Hematol 1997;25:19–25.
5. Gravallese EM, Manning C, Tsay A, Naito A, Pan C, Amento E, et al. Synovial tissue in rheumatoid arthritis is a source of osteoclast differentiation factor. Arthritis Rheum 2000;43:250–8.
6. Yasuda H, Shima N, Nakagawa N, Yamaguchi K, Kinosaki M, Mochizuki S, et al. Osteoclast differentiation factor is a ligand for osteoprotegerin/osteoclastogenesis-inhibitory factor and is identical to TRANCE/RANKL. Proc Natl Acad Sci U S A 1998;95:3597–602.
7. Nakashima T, Hayashi M, Fukunaga T, Kurata K, Oh-Hora M, Feng JQ, et al. Evidence for osteocyte regulation of bone homeostasis through RANKL expression. Nat Med 2011;17:1231–4.
8. Kotake S, Udagawa N, Hakoda M, Mogi M, Yano K, Tsuda E, et al. Activated human T cells directly induce osteoclastogenesis from human monocytes: possible role of T cells in bone destruction in rheumatoid arthritis patients. Arthritis Rheum 2001;44:1003–12.
9. Arai F, Miyamoto T, Ohneda O, Inada T, Sudo T, Brasel K, et al. Commitment and differentiation of osteoclast precursor cells by the sequential expression of c-Fms and receptor activator of nuclear factor κB (RANK) receptors. J Exp Med 1999;190:1741–54.
10. Karmakar S, Kay J, Gravallese EM. Bone damage in rheumatoid arthritis: mechanistic insights and approaches to prevention. Rheum Dis Clin North Am 2010;36:385–404.
11. Maldonado CA, Castagna LF, Rabinovich GA, Landa CA. Immunocytochemical study of the distribution of a 16-kDa galectin in the chicken retina. Invest Ophthalmol Vis Sci 1999;40:2971–7.
12. Egan PJ, van Nieuwenhuijze A, Campbell IK, Wicks IP. Promotion of the local differentiation of murine Th17 cells by synovial macrophages during acute inflammatory arthritis. Arthritis Rheum 2008;58:3720–9.
13. Yarilina A, Xu K, Chen J, Ivashkiv LB. TNF activates calcium-nuclear factor of activated T cells (NFAT)c1 signaling pathways in human macrophages. Proc Natl Acad Sci U S A 2011;108:1573–8.
14. Fujishima S, Hoffman AR, Vu T, Kim KJ, Zheng H, Daniel D, et al. Regulation of neutrophil interleukin 8 gene expression and protein secretion by LPS, TNF-α, and IL-1β. J Cell Physiol 1993;154:478–85.

15. Kinne RW, Stuhlmuller B, Burmester GR. Cells of the synovium in rheumatoid arthritis: macrophages. Arthritis Res Ther 2007;9:224.
16. Firestein GS. The T cell cometh: interplay between adaptive immunity and cytokine networks in rheumatoid arthritis. J Clin Invest 2004;114:471–4.
17. Aarvak T, Chabaud M, Kallberg E, Miossec P, Natvig JB. Change in the Th1/Th2 phenotype of memory T-cell clones from rheumatoid arthritis synovium. Scand J Immunol 1999;50:1–9.
18. Harrington LE, Hatton RD, Mangan PR, Turner H, Murphy TL, Murphy KM, et al. Interleukin 17-producing $CD4^+$ effector T cells develop via a lineage distinct from the T helper type 1 and 2 lineages. Nat Immunol 2005;6:1123–32.
19. Filippin LI, Vercelino R, Marroni NP, Xavier RM. Redox signalling and the inflammatory response in rheumatoid arthritis. Clin Exp Immunol 2008;152:415–22.
20. Reeves EP, Lu H, Jacobs HL, Messina CG, Bolsover S, Gabella G, et al. Killing activity of neutrophils is mediated through activation of proteases by K^+ flux. Nature 2002;416:291–7.
21. Lambeth JD, Krause KH, Clark RA. NOX enzymes as novel targets for drug development. Semin Immunopathol 2008;30:339–63.
22. Henrotin YE, Bruckner P, Pujol JP. The role of reactive oxygen species in homeostasis and degradation of cartilage. Osteoarthritis Cartilage 2003;11:747–55.
23. Garrett IR, Boyce BF, Oreffo RO, Bonewald L, Poser J, Mundy GR. Oxygen-derived free radicals stimulate osteoclastic bone resorption in rodent bone in vitro and in vivo. J Clin Invest 1990;85:632–9.
24. Goldring SR. Pathogenesis of bone erosions in rheumatoid arthritis. Curr Opin Rheumatol 2002;14:406–10.
25. Olofsson P, Holmberg J, Tordsson J, Lu S, Akerstrom B, Holmdahl R. Positional identification of Ncf1 as a gene that regulates arthritis severity in rats. Nat Genet 2003;33:25–32.
26. Hultqvist M, Olofsson P, Holmberg J, Backstrom BT, Tordsson J, Holmdahl R. Enhanced autoimmunity, arthritis, and encephalomyelitis in mice with a reduced oxidative burst due to a mutation in the Ncf1 gene. Proc Natl Acad Sci U S A 2004;101:12646–51.
27. Petrow PK, Thoss K, Henzgen S, Katenkamp D, Brauer R. Limiting dilution analysis of the frequency of autoreactive lymph node cells isolated from mice with antigen-induced arthritis. J Autoimmun 1996;9:629–35.
28. Bremell T, Abdelnour A, Tarkowski A. Histopathological and serological progression of experimental Staphylococcus aureus arthritis. Infect Immun 1992;60:2976–85.
29. Windahl SH, Vidal O, Andersson G, Gustafsson JA, Ohlsson C. Increased cortical bone mineral content but unchanged trabecular bone mineral density in female $ER\beta^{-/-}$ mice. J Clin Invest 1999;104:895–901.
30. Grevers LC, de Vries TJ, Vogl T, Abdollahi-Roodsaz S, Sloetjes AW, Leenen PJ, et al. S100A8 enhances osteoclastic bone resorption in vitro through activation of Toll-like receptor 4: implications for bone destruction in murine antigen-induced arthritis. Arthritis Rheum 2011;63:1365–75.
31. Lawlor KE, Campbell IK, Metcalf D, O'Donnell K, van Nieuwenhuijze A, Roberts AW, et al. Critical role for granulocyte colony-stimulating factor in inflammatory arthritis. Proc Natl Acad Sci U S A 2004;101:11398–403.
32. Lawlor KE, Campbell IK, O'Donnell K, Wu L, Wicks IP. Molecular and cellular mediators of interleukin-1–dependent acute inflammatory arthritis. Arthritis Rheum 2001;44:442–50.
33. Lawlor KE, Wong PK, Campbell IK, van Rooijen N, Wicks IP. Acute CD4+ T lymphocyte–dependent interleukin-1–driven arthritis selectively requires interleukin-2 and interleukin-4, joint macrophages, granulocyte–macrophage colony-stimulating factor, interleukin-6, and leukemia inhibitory factor. Arthritis Rheum 2005;52:3749–54.
34. Ziolkowska M, Koc A, Luszczykiewicz G, Ksiezopolska-Pietrzak K, Klimczak E, Chwalinska-Sadowska H, et al. High levels of IL-17 in rheumatoid arthritis patients: IL-15 triggers in vitro IL-17 production via cyclosporin A-sensitive mechanism. J Immunol 2000;164:2832–8.
35. Tetta C, Camussi G, Modena V, Di Vittorio C, Baglioni C. Tumour necrosis factor in serum and synovial fluid of patients with active and severe rheumatoid arthritis. Ann Rheum Dis 1990;49:665–7.
36. Goto M, Fujisawa M, Yamada A, Okabe T, Takaku F, Sasano M, et al. Spontaneous release of angiotensin converting enzyme and interleukin 1β from peripheral blood monocytes from patients with rheumatoid arthritis under a serum free condition. Ann Rheum Dis 1990;49:172–6.
37. Oelzner P, Brauer R, Henzgen S, Thoss K, Wunsche B, Hersmann G, et al. Periarticular bone alterations in chronic antigen-induced arthritis: free and liposome-encapsulated clodronate prevent loss of bone mass in the secondary spongiosa. Clin Immunol 1999;90:79–88.
38. Omar O, Suska F, Lenneras M, Zoric N, Svensson S, Hall J, et al. The influence of bone type on the gene expression in normal bone and at the bone-implant interface: experiments in animal model. Clin Implant Dent Relat Res 2011;13:146–56.
39. Zhou FH, Foster BK, Zhou XF, Cowin AJ, Xian CJ. TNF-α mediates p38 MAP kinase activation and negatively regulates bone formation at the injured growth plate in rats. J Bone Miner Res 2006;21:1075–88.
40. Kochanowska I, Chaberek S, Wojtowicz A, Marczynski B, Wlodarski K, Dytko M, et al. Expression of genes for bone morphogenetic proteins BMP-2, BMP-4 and BMP-6 in various parts of the human skeleton. BMC Musculoskelet Disord 2007;8:128.
41. Zwerina J, Tuerk B, Redlich K, Smolen JS, Schett G. Imbalance of local bone metabolism in inflammatory arthritis and its reversal upon tumor necrosis factor blockade: direct analysis of bone turnover in murine arthritis. Arthritis Res Ther 2006;8:R22.
42. McCulloch EA, Buick RN, Till JE. Normal and leukemic hemopoiesis compared. Cancer 1978;42:845–53.
43. Banfi G, Iorio EL, Corsi MM. Oxidative stress, free radicals and bone remodeling. Clin Chem Lab Med 2008;46:1550–5.
44. Cedergren J, Forslund T, Sundqvist T, Skogh T. Intracellular oxidative activation in synovial fluid neutrophils from patients with rheumatoid arthritis but not from other arthritis patients. J Rheumatol 2007;34:2162–70.
45. Eggleton P, Wang L, Penhallow J, Crawford N, Brown KA. Differences in oxidative response of subpopulations of neutrophils from healthy subjects and patients with rheumatoid arthritis. Ann Rheum Dis 1995;54:916–23.
46. Kelkka T, Hultqvist M, Nandakumar KS, Holmdahl R. Enhancement of antibody-induced arthritis via Toll-like receptor 2 stimulation is regulated by granulocyte reactive oxygen species. Am J Pathol 2012;181:141–50.
47. Pizzolla A, Hultqvist M, Nilson B, Grimm MJ, Eneljung T, Jonsson IM, et al. Reactive oxygen species produced by the NADPH oxidase 2 complex in monocytes protect mice from bacterial infections. J Immunol 2012;188:5003–11.
48. Sareila O, Kelkka T, Pizzolla A, Hultqvist M, Holmdahl R. NOX2 complex-derived ROS as immune regulators. Antioxid Redox Signal 2011;15:2197–208.
49. Kielland A, Blom T, Nandakumar KS, Holmdahl R, Blomhoff R, Carlsen H. In vivo imaging of reactive oxygen and nitrogen species in inflammation using the luminescent probe L-012. Free Radic Biol Med 2009;47:760–6.
50. Kollias G, Papadaki P, Apparailly F, Vervoordeldonk MJ, Holmdahl R, Baumans V, et al. Animal models for arthritis: innovative tools for prevention and treatment. Ann Rheum Dis 2011;70:1357–62.